ADVANCED MATERIALS
www.advmat.de

Pillar-Assisted Epitaxial Assembly of Toric Focal Conic Domains of Smectic-A Liquid Crystals

Apiradee Honglawan, Daniel A. Beller, Marcello Cavallaro, Randall D. Kamien, Kathleen J. Stebe, and Shu Yang**

Self-assembly, self-processing, and bottom-up design are ever more important tools for the development of new materials of both fundamental and technological interest due to their robust capability for generating complex, hierarchical structures. In general, self-assembling materials, including colloids, block copolymers, and supramolecules or DNA form thermodynamically stable structures over a broad range of length scales, from the micro- to nanoscales. Structure formation in these long-range ordered phases is often governed by entropic and geometric considerations, leading frequently to a limited variety of optimal, close-packed structures. However, close-packed structures are not always appropriate in device applications. Some control has been gained through so-called graphoepitaxy, which exploits substrates with topological[1–5] or chemical[6] surface relief patterns that nearly match the domain structures of block copolymers, for instance, and direct their epitaxial assembly into nanostructures with long-range positional order and orientation in thin films. However, epitaxial assembly of highly ordered square arrays has only been recently achieved in both triblock copolymers[7,8] and supermolecular assemblies of hydrogen-bonding diblock copolymer in thin films.[9]

Because of their geometrical, mechanical, and electronic anisotropy, liquid crystals (LCs) are not only highly sensitive to external aligning fields but can also exquisitely control the propagation of electromagnetic phenomena. Consequently, the patterning of LC molecules has long been of interest for scientific discovery and technological advancement.

Smectic-A (SmA) LCs are characterized by arrangement of molecules into layers with the long molecular axis parallel to the layer normal. When the surface chemistry promotes planar alignment of LC molecules, SmA LCs spontaneously form highly ordered hexagonal arrays of toric focal conic domains (TFCDs)[10] in which smectic layers wrap around a pair of disclination lines formed by a circle and a straight line passing through the circle center. In surface measurements, a defect domain appears as a circular, cone-shaped dimple at the LC/air interface. The bending of the LC layers away from the flat equilibrium SmA to form TFCDs results from the competing effects of planar anchoring at the LC/substrate interface and homeotropic anchoring at the LC/air interface. In the standard smectic ground state, the smectic layers are flat and parallel to the substrate and thus the molecular orientation points normal to both the LC/air and LC/substrate interfaces. The TFCDs form spontaneously when the decrease in surface energy obtained by planar anchoring on the substrate outweighs the elastic energy cost of bending the layers and the increase in surface energy due to the dimple-like deformation of the LC/air interface. Regular hexagonal lattices of TFCDs have been used to create microlens arrays,[11] matrices for the self-assembly of soft microsystems,[12–14] lithographic templates,[15] 2D charge transport models,[16] and patterned functional surfaces. The ability to control the size and arrangement of TFCDs is currently under investigation; for instance, studies have employed substrates presenting different surface chemistries,[16–19] confinement within 1D microchannels,[16,20–23] and randomly patterned planar and depressed substrates.[24] Little is known, however, about a higher level of control of TFCDs into three dimensions.[25,26] Controlling topological defects and smectic LC phases in three dimensions is of particular interest to the generation of blue phases and other topologically structured materials, which will lead to possibly disruptive display technologies.

Here, we demonstrate the epitaxial assembly of SmA LCs into arrays of TFCDs with variable sizes and arbitrary symmetries (e.g., a square lattice) directed by pillar arrays. We utilize materials that induce planar anchoring of LC molecules, such as SU-8, a bisphenol A epoxy derivative. By varying the pillar dimensions (size, height, and spacing) and thickness of the LC film, we can confine and direct the growth of each TFCD. As a result, we promote a new variety of TFCD arrays beyond the close-packed hexagonal arrangement formed spontaneously on a flat surface by controlling the size and symmetry of the underlying pillar pattern. We hope that this template-directed assembly method will benefit a number of engineering applications and advanced device concepts.

The LCs used here are rigid biphenyl molecules with semifluorinated chains (see chemical structure in Figure S1, Supporting Information). They have a smectic-A LC phase at ≈114 °C, and retain TFCD structure when quenched to

A. Honglawan, M. Cavallaro, Prof. K. J. Stebe, Prof. S. Yang
Department of Chemical and Biomolecular Engineering
University of Pennsylvania
Towne Building, 220 South 33rd Street,
Philadelphia, PA 19104, USA
E-mail: shuyang@seas.upenn.edu
D. A. Beller, Prof. R. D. Kamien
Department of Physics and Astronomy
University of Pennsylvania
209 South 33rd Street,
Philadelphia, PA 19104, USA
E-mail: kamien@physics.upenn.edu
Prof. S. Yang
Department of Materials Science and Engineering
University of Pennsylvania
3231 Walnut Street, Philadelphia, PA 19104, USA

DOI: 10.1002/adma.201103008

ADVANCED MATERIALS
www.advmat.de

Materials Views
www.MaterialsViews.com

room temperature. The LCs were synthesized by a two-step reaction following the literature,[27,28] and their structure was confirmed by Fourier transform infrared (FT-IR) spectroscopy and ^{1}H NMR (see Supporting Information). Highly ordered hexagonal arrays of TFCDs were observed on bare Si wafers and SU-8 coated Si wafers via scanning electron microscopy (SEM) with corresponding Maltese cross patterns in polarized optical microscopy (POM) (see Figure S3a–c, Supporting Information). The same morphology has been reported by Kim et al.[23] on Teflon amorphous fluoropolymer coated Si and glass substrates, suggesting high planar anchoring strength of the LCs on these substrates. It has been suggested that the TFCD radius *a*, measured as half of the center-to-center distance between neighboring TFCDs, is roughly equal to half of the LC film thickness (*h*) in these regions.[23,24] In our system, the average TFCD radius <*a*> on the flat Si and SU-8 surface is ≈2.5 μm for $h = 5$ μm, in agreement with the literature.

Using 1D microchannels, Kim et al. studied confined assembly of high density TFCDs and reported that domain formation was strongly influenced by both the channel width (*W*) and, even more dramatically, by the channel depth (*H*).[23] They found that an energetically stable, hexagonal array of TFCDs is formed when *W* and *H* are above the critical values, $W_c \approx 4$ μm and $H_c \approx 2$ μm.[23] Here, we use SU-8 pillar arrays with varying pillar diameter, height, spacing, and symmetry as a 3D confinement system for SmA LCs.

Figure 1,**2** demonstrate different TFCD morphologies from the assembly of SmA LCs directed by confinement and interaction with the underlying square pillar arrays at variable length scales. The geometry created by a square array of pillars is described by three parameters: *S*, the smallest distance between the edges of two diagonally neighboring pillars; *D*, the pillar diameter; and *H*, the pillar height. Depending on the values of these parameters and of the LC thickness *h*, the pillars define anchoring points for TFCDs at the centers of the pillars' top surfaces, or on the substrate positioned symmetrically between four neighboring pillars, or both.

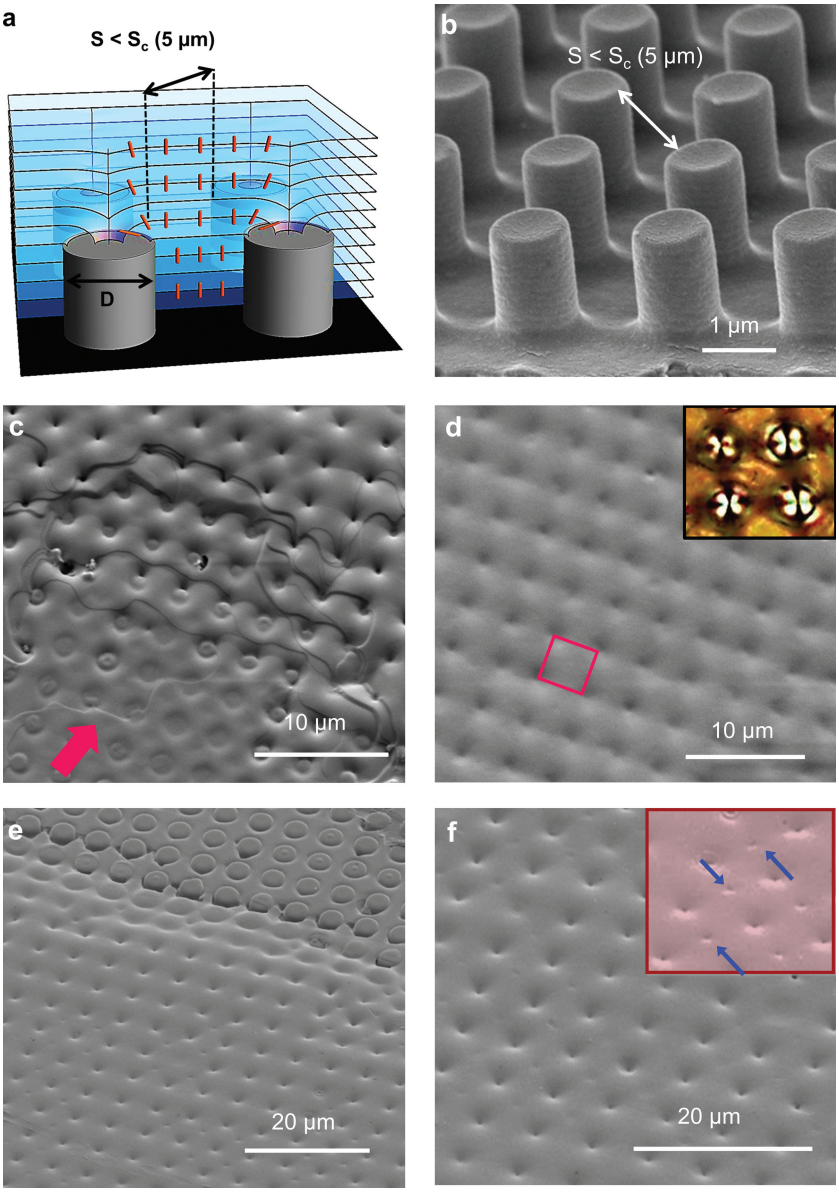

Figure 1. Epitaxial assembly of TFCDs on SU-8 square pillar arrays with diagonal separation $S < S_c$ (the critical value of *S*). a) Schematic illustration of SmA LCs confined by a SU-8 square pillar array with $S < S_c$. b) SEM image of the SU-8 square pillar array with diameter $D = 1$ μm, diagonal separation $S = 3$ μm, and height $H = 1.5$ μm. c,d) SEM images of the corresponding TFCDs assembled on the SU-8 pillar array (b) at various LC thicknesses, $h = 1.5$–2.5 μm (c) and 3.5 μm (d). Inset of (d): POM image at a high magnification. e,f) SEM images of TFCDs assembled on the SU-8 pillar array with $D = 5$ μm, S (≈S_c) = 5 μm, $H = 2.5$ μm at various LC thickness, $h = 2.5$–4 μm (e) and 4.0 μm (f). Inset of (f): high magnification. The blue arrows indicate satellite TFCDs formed between the neighboring pillars.

When the LC thickness *h* exceeds the pillar height *H* by at least 1.5 μm, a single TFCD forms on the circular top of each pillar (see Figure 1a). Figure 1c and Figure S5c (Supporting Information) show an area of unleveled LC thickness on pillar arrays, clearly revealing that the top surface of each pillar defines an anchoring point of one TFCD. No TFCDs were observed on the top of pillars, however, when $D < 1$ μm. This is due to inadequate anchoring area for a circular defect. For such small TFCD diameters, the negative energy contribution from the surface term at the LC-substrate boundary is outweighed by the elastic energy cost and the increased surface area at the air-LC interface. The experimental value of this critical diameter, $D_c \approx 1$ μm, agrees well with our calculations of TFCD energies in 3D pillar arrays (see details in the Supporting Information), which

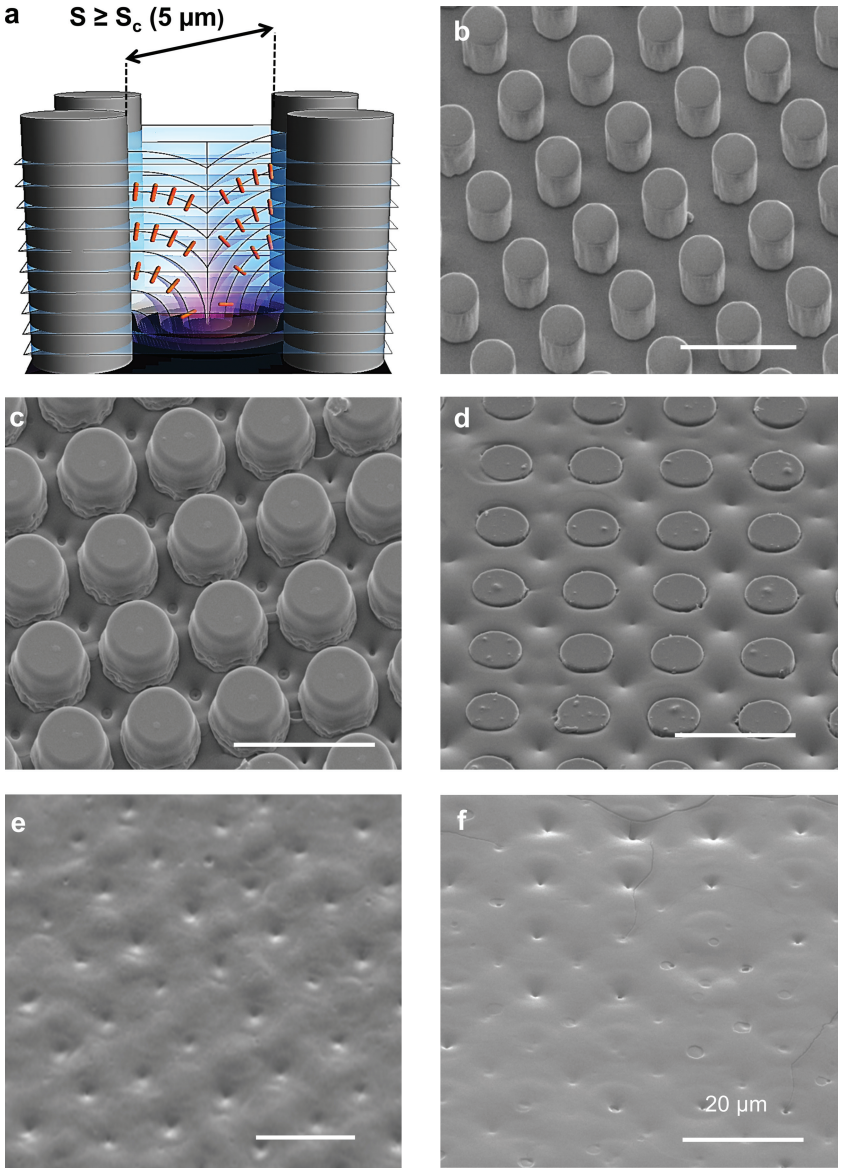

Figure 2. Epitaxial assembly of TFCDs on SU-8 square pillar arrays with diagonal separation $S \geq S_c$ and diameter $D \geq D_c$ (the critical value of D). a) Schematic illustration of SmA LCs confined by a SU-8 square pillar array with S ‡!S$_c$ and $D \geq D_c$. b) SEM image of a SU-8 square pillar array with diameter $D = 10$ μm, diagonal separation $S = 15$ μm, and height $H = 7.5$ μm. c–f) The corresponding TFCDs assembled on the SU-8 pillar array (b) at various LC thicknesses: $h = 2$ μm (c), 7.5 μm (d), 8 μm (e), and 9 μm (f).

predict the minimum domain diameter of an energetically stable TFCD to be 1.0 μm. Notably, this critical diameter does not change over a wide range of $h - H$. Thus, with directing pillars of $D \geq D_c$, a square array of TFCDs could be generated that grows into the bulk. Indeed, we find that both the square symmetry and dimension of the pillar array was maintained in the TFCDs for LC thicknesses up to 40 μm (see Figure S4, Supporting Information), demonstrating the long-range ordering into the bulk from surface epitaxy. Since the main aim of our study is to control the arrangements of TFCDs other than the natural close-packed structures using geometric confinement by pillars, in all experiments we avoided making both D and $h - H$ so large as to generate multiple close-packed TFCDs on the top surface of a single pillar.

Our experimental data also show that the pillar array defines TFCD anchoring points on the substrate between pillars: in the center of each unit cell defined by four neighboring pillars, a single TFCD is observed when the diagonal pillar spacing S exceeds a critical value, $S_c \approx 5$ μm, and the LC thickness h exceeds the critical height, $h_c \approx 1.5$ μm. The pillars cause this transition in two ways: they limit the surface area on the substrate available to the TFCD for planar anchoring and they impose additional planar anchoring conditions along the vertical pillar sides, requiring the smectic layers to orient horizontally as they approach the pillars. As a result, when $S < S_c$, LC layers align parallel to the bottom of the substrate, filling up the spaces between pillars without forming a defect domain at any LC thickness, as shown in Figure 1c (region marked with an arrow), where $S = 3$ μm $< S_c$ and $h = 1.5$ μm $\approx h_c$. Conversely, TFCDs formed between the pillars when $S = 15$ μm $> S_c$ for $h \geq h_c$, as shown in Figure 2c,d. When $S \geq S_c$, $D \geq D_c$, and h surpasses the pillar height H by at least 1.5 μm (i.e., $h - H \geq h_c$), TFCDs are observed to develop from both anchoring sites, the surface between pillars and the top surface of the pillars, as shown in Figure 2f. Square lattices of TFCDs between pillars were observed for H as low as 0.5 μm; therefore, the critical pillar height H_c, which marks the transition from a hexagonal close-packed lattice of TFCDs to a square lattice, must be at a smaller length scale but, presumably, much greater than the layer spacing (3.2 nm).

It is noted that the formation of the TFCDs was not only influenced by the geometry of the pillar array alone, but also the surface chemistry of the confinement. From an energetic standpoint, the formation of TFCDs in a thin-film smectic LC requires surface chemistry that promotes planar alignment of LCs, as provided by materials such as SU-8, a widely used photoresist to fabricate high-aspect-ratio pillar arrays. Otherwise, there would be no TFCD developed within the confinement at any dimension. The importance of surface chemistry is further strikingly demonstrated when the SU-8 pillar arrays are coated with Au, as a result of which no TFCDs form (see Figure S6, Supporting Information). To this point, our results clearly demonstrate that this geometric 3D confinement of SU-8 pillars essentially permits the controlled growth of the multiscale TFCD array, which is not achievable through a simple 1D patterning approach.

At the critical spacing, $S \approx S_c$ (5 μm), Figure 1e,f reveal evidence of coexistence between TFCDs on the substrate

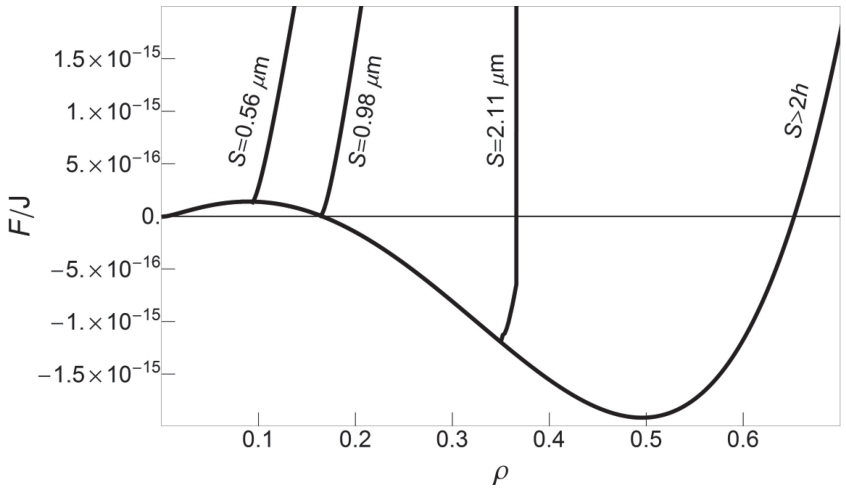

Figure 3. Calculated TFCD energy relative to the flat-layer state versus $\rho = a/h$ using $h = H = 3.0$ μm, $D = 1$ μm, and varying pillar spacing with diagonal separation S. A sharp energy penalty is evident for TFCDs whose diameter exceeds S, while smaller sized TFCDs have the same energy as on a flat substrate. Materials constants for calculation[23] include the splay elastic constant $K = 5 \times 10^{-11}$ N, the defect core size $\xi = 3 \times 10^{-9}$ m, and the energy per unit area for molecules oriented normal to the LC/air interface $\sigma_{\perp}^{air} = 20 \times 10^{-3}$ N m^{-1}. The energy per unit area for molecules oriented parallel vs. normal to the LC/SU-8 interface is determined $\Delta\sigma^{subs} = -1.1 \times 10^{-3}$ N m^{-1}. This is found by requiring that the calculated TFCD energy allow energetically stable TFCDs only for values of $h \geq h_c = 1.5$ μm.

between pillars (the small dimples indicated by blue arrows in Figure 1f) and the flat-layer state, where no dimple forms in the surface between pillars. This coexistence may be due to kinetics preventing complete equilibration. The inconsistency with which TFCDs form between pillars in Figure 1e,f is to be contrasted with the nearly perfect square array of TFCDs that form on top of the pillars in the same images. The TFCDs on top of the pillars exhibit a larger dimple in the surface because they are centered at a lesser depth below the surface. Indeed, our calculations (**Figure 3**) of smectic bending and surface energies predict that when the LC is confined within a space smaller than a critical spacing, homeotropic alignment of molecules at the substrate surface becomes energetically preferable to the formation of a TFCD between pillars. The predicted S_c is, however, ≈1 μm. The discrepancy between experiment and theory may arise from our assumption that the smectic layers distort only within the TFCD (see detailed discussion in Supporting Information, Figure S7–S10), so that there is an energy penalty only when the TFCD comes into contact with the pillar. Through this assumption, we have ignored more complicated layer organization that may occur at the sharp corner where the pillar meets the substrate and the boundary conditions change rapidly. Such structures could allow the pillars to effectively "repel" TFCDs at a distance. Further experimentation will be pursued to test the influence of sharp corners of pillars.

It is interesting that only single domains appear in the space between four neighboring pillars at any LC thickness even though multiple domains having equilibrium diameter roughly equivalent to h were expected for sufficiently large S (≈15 μm) and low LC thickness as, for instance, $h = 2$ μm (Figure 2c). Our experimental results suggest that the topographical confinement effect of pillars remains influential for LC alignment at this length scale, although it is also possible that the variation in both surface chemistry and curvature of each pillar could lead to a varying anchoring strength of LC on the substrate, which would result in larger domains.

Our results demonstrate three important features with regard to epitaxial assembly of LC molecules confined and directed by an SU-8 pillar array. First, it is possible to alter the naturally occurring close-packed lattice of the TFCD arrays via anchoring. To further confirm the control of TFCD arrangement by the supporting pillars, we confined the LCs on a hexagonal pillar array with $D = 1$ μm, $S = 1$ μm, and $H = 2$ μm (**Figure 4**a). As anticipated, the top surface of the underlying pillars served as anchoring points of the TFCDs, resulting in a hexagonal array of the defect domains with a domain diameter of ≈1 μm, equal to S (see Figure 4b,c).

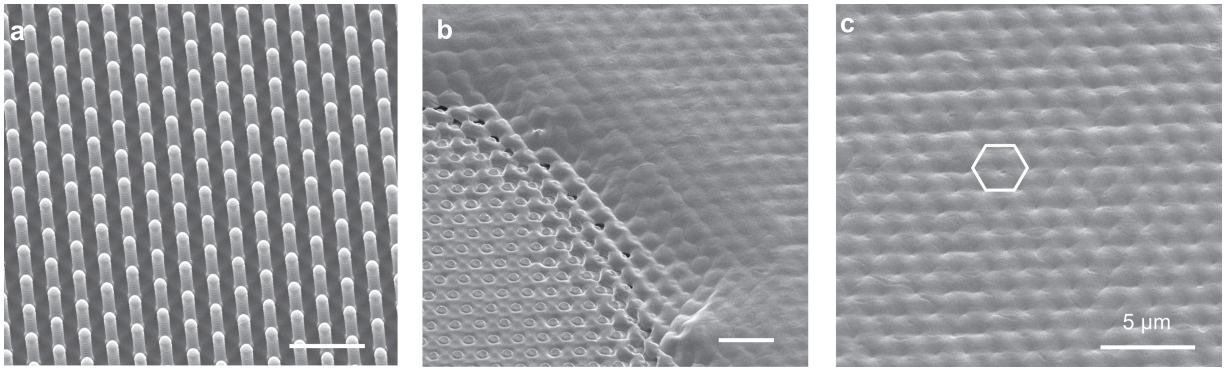

Figure 4. Epitaxial assembly of TFCDs on SU-8 hexagonal pillar arrays. a) SEM images of the SU-8 hexagonal pillar array with diameter $D = 1$ μm, diagonal separation $S = 1$ μm, height $H = 2$ μm. b,c) The corresponding TFCDs on the hexagonal pillar array (a) at various LC thickness vs. pillar height, $h - H = 0$–8 μm (b) and 8 μm (c).

Second, defect size and spacing can be controlled simply by varying the dimensions of the directing pillars, which enables generation of TFCD arrays with defect size and spacing smaller than previously observed in the same material at any given LC thickness (≈5 μm on treated and untreated flat Si surfaces and ≈2.6 μm in a 1D microchannel[24] for the smallest tested h = 5 μm). The possibility of down-scaling the spacing between defects will be beneficial especially for LC-based device fabrication.

The third and most important implication of pillar directed epitaxial assembly of LCs is the conservation of the symmetry and dimension of TFCD arrays at high LC thickness, experimentally observed up to 40 μm despite the fact that on a flat non-patterned substrate the domain size scales as the film thickness.[24,29] This behavior is a direct result of LC confinement and epitaxial growth of individual TFCDs in which the geometry of the pillar sets the upper limit for the size of a domain by imposing a sharp energy barrier to further domain growth. Furthermore, the minimum allowable domain size is also independent of LC thickness, as predicted by the energy model: in Figure S7 (Supporting Information), we plot the calculated energy of a TFCD relative to the flat-layer state as a function of domain radius. The energy curve crosses zero at approximately the same domain radius (0.5 μm) at any $h \geq$ 2 μm, setting S_c and D_c independent of h. Our results are further supported by the observation of smectic 8CBs assembled on a circularly patterned flat substrate,[24] where the diameter of the TFCDs is determined solely by the diameter of the circular units regardless of the film thickness. As a result, the simple proof-of-principle experiments presented here together with modeling provide a viable technique to generate a uniform array with arbitrary symmetry of equal-sized TFCDs that extend into the bulk.

We have demonstrated epitaxial assembly of SmA LCs using top-down fabricated polymer pillar arrays. The 3D nature of the pillar array is crucial to confine and direct the formation of toric focal conic domains on the top of each pillar as well as between neighboring pillars. Independent of LC thickness (above a critical thickness h_c), the pattern of SU-8 pillar arrays determined the final crystal habit of the TFCD array: both highly ordered square and hexagonal array TFCDs were obtained. The epitaxial approach presented here offers an entirely new and promising organizational principle for smectic LC systems using simple topographic substrates. In turn, it may lead to the formation of more complex LC phases in 3D that are critical to the advancement of LC-based electronic and optical devices,[25,26] and perhaps generation of novel materials when incorporating functional units such as nanoparticles, nanocrystals, and carbon nanotubes into the LC layers.

Supporting Information

Supporting Information is available from the Wiley Online Library or from the author.

Acknowledgements

This work is supported by National Science Foundation (NSF) MRSEC grant DMR05-20020, and NSF CAREER award DMR-0548070 (S.Y.). The authors acknowledge Professor Paul Heiney (Penn/Physics) for X-ray scattering study to confirm the LC phases and the Penn Regional Nanotechnology Facility (PRNF) for access to SEM imaging.

Received: August 5, 2011
Revised: September 7, 2011
Published online: October 17, 2011

[1] R. A. Segalman, H. Yokoyama, E. J. Kramer, *Adv. Mater.* **2001**, *13*, 1152.
[2] S. O. Kim, H. H. Solak, M. P. Stoykovich, N. J. Ferrier, J. J. de Pablo, P. F. Nealey, *Nature* **2003**, *424*, 411.
[3] M. P. Stoykovich, M. Müller, S. O. Kim, H. H. Solak, E. W. Edwards, J. J. de Pablo, P. F. Nealey, *Science* **2005**, *308*, 1442.
[4] I. Bita, J. K. W. Yang, Y. S. Jung, C. A. Ross, E. L. Thomas, K. K. Berggren, *Science* **2008**, *321*, 939.
[5] H. Arora, P. Du, K. W. Tan, J. K. Hyun, J. Grazul, H. L. Xin, D. A. Muller, M. O. Thompson, U. Wiesner, *Science* **2010**, *330*, 214.
[6] E. W. Edwards, M. F. Montague, H. H. Solak, C. J. Hawker, P. F. Nealey, *Adv. Mater.* **2004**, *16*, 1315.
[7] C. B. Tang, J. Bang, G. E. Stein, G. H. Fredrickson, C. J. Hawker, E. J. Kramer, M. Sprung, J. Wang, *Macromolecules* **2008**, *41*, 4328.
[8] V. P. Chuang, J. Gwyther, R. A. Mickiewicz, I. Manners, C. A. Ross, *Nano Lett.* **2009**, *9*, 4364.
[9] C. B. Tang, E. M. Lennon, G. H. Fredrickson, E. J. Kramer, C. J. Hawker, *Science* **2008**, *322*, 429.
[10] P. G. De Gennes, J. Prost, *The Physics of Liquid Crystals*, Clarendon Press, Oxford **1993**.
[11] Y. H. Kim, H. S. Jeong, J. H. Kim, E. K. Yoon, D. K. Yoon, H.-T. Jung, *J. Mater. Chem.* **2010**, *20*, 6557.
[12] L. J. Martinez-Miranda, K. K. Lynn, *J. Appl. Phys.* **2009**, *105*, 084305.
[13] R. Pratibha, W. Park, I. I. Smalyukh, *J. Appl. Phys.* **2010**, *107*, 063511.
[14] D. K. Yoon, M. C. Choi, Y. H. Kim, M. W. Kim, O. D. Lavrentovich, H.-T. Jung, *Nat. Mater.* **2007**, *6*, 866.
[15] Y. H. Kim, D. K. Yoon, H. S. Jeong, H.-T. Jung, *Soft Matter* **2010**, *6*, 1426.
[16] T. D. Choudhury, N. V. S. Rao, R. Tenent, J. Blackburn, B. Gregg, I. I. Smalyukh, *J. Phys. Chem. B* **2010**, *115*, 609.
[17] B. Zappone, E. Lacaze, H. Hayeb, M. Goldmann, N. Boudet, P. Barois, M. Alba, *Soft Matter* **2010**, *7*, 1161.
[18] B. Zappone, E. Lacaze, *Phys. Rev. E* **2008**, *78*, 061704.
[19] K. A. Simon, E. A. Burton, F. Cheng, N. Varghese, E. R. Falcone, L. Wu, Y.-Y. Luk, *Chem. Mater.* **2010**, *22*, 2434.
[20] M. C. Choi, T. Pfohl, Z. Wen, Y. Li, M. W. Kim, J. N. Israelachvili, C. R. Safinya, *Proc. Natl. Acad. Sci. USA* **2004**, *101*, 17340.
[21] D. K. Yoon, R. Deb, D. Chen, E. Körblova, R. Shao, K. Ishikawa, N. V. S. Rao, D. M. Walba, I. I. Smalyukh, N. A. Clark, *Proc. Natl. Acad. Sci. USA* **2010**, *107*, 21311.
[22] R. Mitya, W. Bentley, A. H. Mark, J. B. Philip, *J. Appl. Phys.* **2008**, *104*, 044902.
[23] Y. H. Kim, D. K. Yoon, M. C. Choi, H. S. Jeong, M. W. Kim, O. D. Lavrentovich, H.-T. Jung, *Langmuir* **2009**, *25*, 1685.
[24] W. Guo, S. Herminghaus, C. Bahr, *Langmuir* **2008**, *24*, 8174.
[25] B. A. DiDonna, R. D. Kamien, *Phys. Rev. Lett.* **2002**, *89*, 215504.
[26] B. A. DiDonna, R. D. Kamien, *Phys. Rev. E* **2003**, *68*, 041703.
[27] G. Johansson, V. Percec, G. Ungar, J. P. Zhou, *Macromolecules* **1996**, *29*, 646.
[28] V. Percec, G. Johansson, G. Ungar, J. Zhou, *J. Am. Chem. Soc.* **1996**, *118*, 9855.
[29] W. Guo, C. Bahr, *Phys. Rev. E* **2009**, *79*, 011707.